European Polymer Journal 189 (2023) 111961

Contents lists available at ScienceDirect

European Polymer Journal

journal homepage: www.elsevier.com/locate/europolj

Hofmeister series: An insight into its application on gelatin and alginate-based dual-drug biomaterial design

Sougat Das, Lopamudra Giri, Saptarshi Majumdar *

Department of Chemical Engineering, Indian Institute of Technology Hyderabad, Telangana 502285, India

ARTICLE INFO

Keywords:
Hofmeister series
Salt anions
Alginate
Gelatin
Interactions

ABSTRACT

Alginate and gelatin are bio-polymers widely used in drug delivery. A range of salts can be used to achieve the required flexibility in biomaterial design. Hofmeister series gives an idea about the behaviour of salts with proteins. However, its application for the design of biomaterials and their specific effect on high-viscosity polymers and polymer mixtures has not quite been explored. Firstly, this work proposes a strategic interaction-based approach for designing a dual-drug ocular biomaterial. Secondly, the impact of different salt anions on gelatin and alginate mixture for the developed protocols is studied by a proposed method of determining shear-dependent general intrinsic viscosity. Thirdly, shear-dependent intrinsic viscosity is used to determine the interaction amongst the polymers in their mixture, which is then correlated to the release profiles and hydrodynamic radii of polymer mixtures. It is observed that Hofmeister anions behave reversely for high-viscosity negatively charged polymers and depends on the charge densities of the anions. For the polyelectrolyte/polyampholyte complex/mixture, the interactions depend on the addition sequence. It is inferred that the kosmotropes are preferred for protocols where salt is added between gelatin and alginate and chaotropes for protocols where salt is added to the gelatin and alginate complex/mixture in terms of release profiles.

1. Introduction

Polymer-based ophthalmic formulations are a novel approach that has been considered in recent times. Chitosan, gellan gum, gelatin, PEG, and Carbopol are some of the polymers that have grabbed the attention of researchers. These formulations result in systemic absorption of the drugs to the site of action, thus reducing the side effects with slow and extended release and increasing the bioavailability [1].

Alginate is a natural, biocompatible, and biodegradable polysaccharide. It forms an in-situ gel in the presence of divalent ions (Ca^{2+} and Mg^{2+}) in the tear fluid [2]. Alginate-based hydrogel beads [3,4], microspheres [5,6], and nanoparticles [7,8] have been investigated to prepare drug delivery vehicles. However, there are few pieces of literature available for ophthalmic formulations. Moreen et al. prepared an in-situ gel using a combination of gum extracted from *Terminalia arjuna* bark resin and alginate for the ophthalmic delivery of moxifloxacin HCl [9]. Another in-situ gel was prepared using a mixture of chitosan and sodium alginate for the ocular delivery of levofloxacin [10]. Liu et al. prepared alginate and HPMC-based formulation for the ophthalmic delivery of gatifloxacin [11]. Gelrite and alginate mixture can also be used to prepare an ion-activated in-situ gelling vehicle to deliver matrine [12]. Séchoy et al. prepared another formulation using alginate to deliver carteolol [13]. Another alginate [14] and a combination of Pluronic F-127 and alginate [15]-based formulations were developed for the ocular delivery of pilocarpine.

Salts are used for inducing the screening of charges on polymer backbones. Screening these charges leads to reducing the viscosity of the formulations to the required limit (60–65 cP at the ocular surface temperature). These salts have different interactions based on their hydration properties. The Hofmeister series categorises different anions and cations according to their protein precipitation ability.

There have been different applications of the Hofmeister series. One such application is to design thermally reversible microgels of poly(N-Isopropylacrylamide) [16]. The effect is also studied on thermoresponsive poly (propylene oxide) [17] and the self-organization of 1-decyl-3-methylimidazolium chloride [18]. Another work shows an application of these anions on the micellization and micellar growth of the surfactant cetylpyridinium chloride [19]. Another study shows the Hofmeister effects on the Thermoresponsive behavior of poly(3-methylene-2-pyrrolidone) derivatives [20]. The chaotropic and

* Corresponding author.
E-mail address: saptarshi@che.iith.ac.in (S. Majumdar).

https://doi.org/10.1016/j.eurpolymj.2023.111961
Received 3 November 2022; Received in revised form 26 February 2023; Accepted 28 February 2023
Available online 4 March 2023

kosmotropic effect on the swelling and compressive elasticity is also evaluated for N-(alkyl)acrylamide-based semi-IPN hybrid gels reinforced with silica nanoparticles [21]. There also have been different research on the effect of salts in polymer brushes [22–28]. However, to the best of our knowledge, no literature has shown an application of the Hofmeister anions in drug release studies analogous to their interactions on the polymer chains. Several choices of salt also allow certain flexibility in designing biomaterial for a targeted application. This article tries to fill this void in the literature along with the development of a dual drug anti-glaucoma formulation.

The Hofmeister anion series (near the isoelectric point) is as follows: $CO_3^{2-} > Citrate^{3-} > SO_4^{2-} > S_2O_3^{2-} > H_2PO_4^- > CH_3COO^- > F^- > Cl^- > Br^- > NO_3^- > I^- > ClO_4^- > SCN^-$. The anions before Cl^- are known as kosmotropes and after Cl^- are known as chaotropes. The kosmotropes promote protein aggregation, reducing its solubility and the opposite effect is true for chaotropes [29–35]. The interaction of kosmotropic anions with water is higher than chaotropes due to their higher hydrodynamic radii (R_H). The chaotropic anions can interact with the amide bonds of the proteins, whereas the kosmotropes get repelled by the peptide backbones [36–39]. This series's full or partial reversal is seen with the change of surface charge from negative to positive with the change in pH [40,41].

The present article concentrates on the interactions of the different anions with the gelatin and alginate system while developing a dual drug anti-glaucoma alginate-based formulation using interactions study as a strategic approach for its design. The interactions are defined in terms of the changes in the hydrodynamic radius (R_H), zeta potential and viscosity with the sequential addition of the formulation components. An increase in R_H with the addition of a component infers its ability to diffuse inside the chains, thus, resulting in a better release. A decrease shows the inability to diffuse, resulting in an inferior release. The zeta potential provides an idea about the overall charge of the ionic system. For positively charged systems, the reduction in zeta potential relates to the screening of the charges in polymers resulting in the collapse of chains, whereas an increase in zeta potential relates to an increased repulsion resulting in chain expansion. For negatively charged systems, the reduction in zeta potential relates to an increased negative charge and thus repulsions inferring the expansion in the chains. An increase in zeta infers the screening of the charges in polymers resulting in the collapse of chains. The viscosity gives another aspect of determining the collapse of chains (decrease in viscosity) and expansion of chains (increase in viscosity due to entanglement of polymer chains). The aim of this work is threefold. Firstly, it focuses on the above interactions between the different constituents of the formulation for the designing of a gelatin and alginate-based biomaterial for the ocular delivery of timolol maleate and latanoprost which is taken as a model system for this study. NaCl is taken as a basis for this study to design four protocols for developing the biomaterial. Secondly, two kosmotropes (Na_2SO_4, CH_3COONa) and two chaotropes (NaCl and $NaNO_3$) and their effect on the four developed protocols are selected for this study to conclude their effect on the biomaterial design and gelatin & alginate complex/mixture. The drug release profiles for these salts are also compared with three release kinetic models (zero order model, first order model and Higuchi model) to provide a better explanation. The constituents for the formulations are also well within the FDA-approved components. The article also proposes a methodology to study the variation in shear-dependent general intrinsic viscosity to determine the interactions amongst the polymers in the mixture with the addition of different salts (for developed formulation protocols). It is correlated with the changes in R_H, thus giving another perspective for the interactions amongst the polymers in the mixture with different salts, which further helps explain the drug release profiles. This work also sheds light on the variation in the Hofmeister series for a high-viscosity negatively charged polyelectrolyte (alginate) and the polyampholyte and polyelectrolyte mixture (gelatin and alginate). Finally, the interactions of these anions with the high viscosity negatively charged polyelectrolyte is also discussed.

2. Experimental section

2.1. Materials

High-viscosity sodium alginate and β - cyclodextrin was purchased from Alfa Aeser. Gelatin was purchased from Sigma Aldrich. NaCl was purchased from SRL chemicals. Timolol maleate and latanoprost were acquired from TCI chemicals.

2.2. Fabrication of dual drug formulations

Gelatin (1 % w/v) was dispersed in water at 40 °C under continuous stirring for 30 mins to ensure complete dissolution. The solution was then cooled to room temperature. Based on the different methodologies, either salt (1% w/v) or timolol maleate (1.65 mg/mL) was added. Sodium alginate (0.4% w/v) was added to the solution and stirred for 30 min, followed by 30 min of ultrasonication. β-cyclodextrin (0.2 % w/v) was then added to the mixture, followed by latanoprost (1.5 μg/mL) and 0.2% w/v sodium alginate. NaOH was then added to increase the pH of the formulation to the physiological level. Different protocols were designed by varying the sequence of NaOH and salt. The different protocols considered for the preparation of the formulations are discussed in section 3.

2.3. Measurement of hydrodynamic radius (R_H)

The polymer solutions are a type of colloidal solutions which exhibits Brownian motion. The light scattered from a suspension of Brownian motion exhibits intensity fluctuations. These fluctuations are related to the diffusivity of the Brownian particles, which is further related to the size of the particles by Stoke-Einstein's equation. The intensity auto correlation function is used to relate these time scale fluctuations of Brownian motion which is as follows [42]:

$$G_\tau^{(2)} = < I(t).I(t+\tau) > \quad (1)$$

where, I(t) is the scattered light intensity and τ is the delay between two time points.

The normalized light intensity ACF $\left(g_\tau^{(2)}\right)$ and the normalized electric field ACF $\left(g_\tau^{(1)}\right)$ are related by Siegert relation as

$$g_\tau^{(2)} = 1 + \beta\left|g_\tau^{(1)}\right|^2 \quad (2)$$

where, β is the coherence factor.

Now, the electric field ACF is expressed as

$$g_\tau^{(1)} = \exp(-\Gamma\tau) \quad (3)$$

Where, Γ is the decay constant and,

$$\Gamma = D_T q^2 \quad (4)$$

where D_T is the translational diffusion coefficient and q is the scattering vector.

Now,

$$g_\tau^{(2)} = 1 + \beta e^{-2\Gamma\tau} \quad (5)$$

which can be substituted as

$$g_\tau^{(2)} = 1 + \beta e^{-2D_T q^2 \tau} \quad (6)$$

which is the correlation function and connects the particle motion with the measured fluctuations. The obtained D_T can be used to measure the hydrodynamic radius (R_H) by relating it with Stoke-Einstein's equation, i.e.,

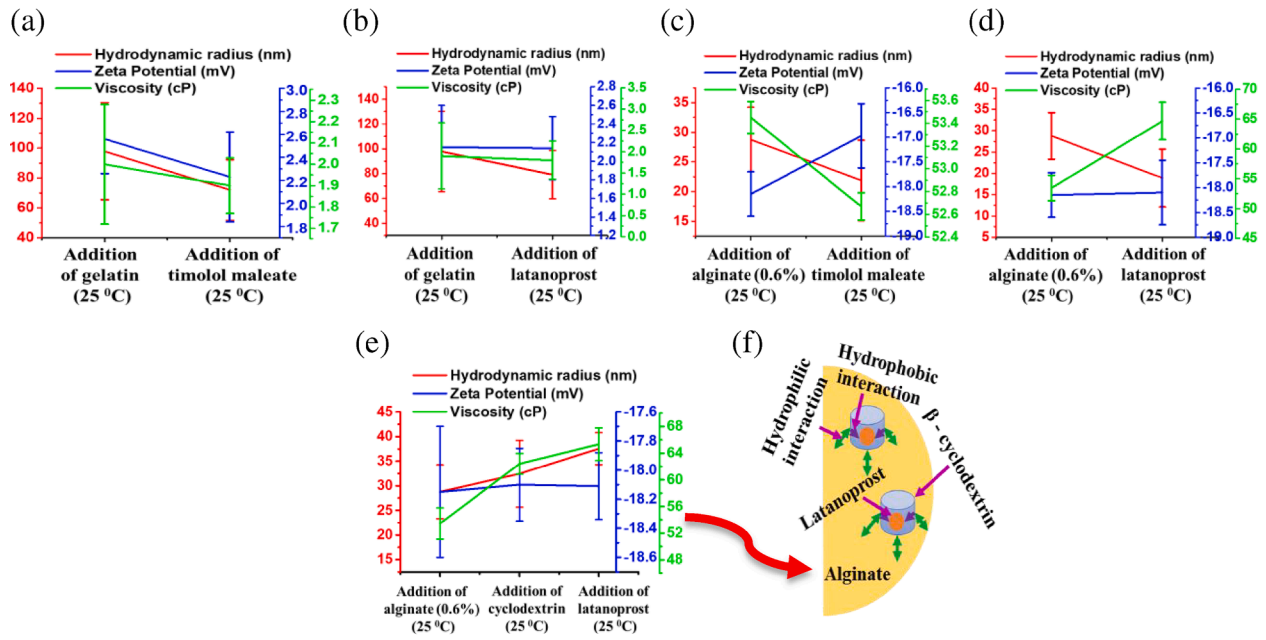

Fig. 1. Interactions between timolol maleate, latanoprost and polymers and alginate, cyclodextrin and latanoprost a) Changes in RH, zeta potential and viscosity with the addition of timolol maleate to gelatin solution, b) Changes in RH, zeta potential and viscosity with the addition of latanoprost to gelatin solution, c) Changes in RH, zeta potential and viscosity with the addition of timolol maleate to alginate solution, d) Changes in RH, zeta potential and viscosity with the addition of latanoprost to alginate solution, e) Changes in RH, zeta potential and viscosity with the addition of β- cyclodextrin followed by latanoprost to alginate solution, f) a rough schematic of the interactions of β- cyclodextrin, alginate and latanoprost.

$$R_H = \frac{kT}{6\pi\eta D_T} \quad (7)$$

where k is the Boltzmann constant, T is temperature, η is the viscosity measured using a rheometer, D_T is the diffusion coefficient measured using the particle size analyzer dynamic light scattering: particle size analyzer (Beckman Coulter Delsa Nano C), and R_H is the hydrodynamic radius. The studies were conducted at 25 °C. All the measurements were performed in triplicates.

2.4. Measurement of zeta potential

The zeta potential of the samples was measured on a dynamic light scattering: zeta potential analyzer (Beckman Coulter Delsa Nano C). The studies were conducted at 25 °C. All measurements were performed in triplicates.

2.5. Rheology studies

The viscosity studies were conducted on a rheometer (Anton Paar, MCR 92). The viscosity of the samples was measured at 25 °C. A shear rate of 100/s was considered for the viscosity studies. All measurements were performed in triplicates.

2.6. Fourier transform infrared spectroscopy/Attenuated total reflectance (FTIR-ATR)

The FTIR-ATR analysis of the liquid samples was performed using Bruker Tensor 37, MIRacle Single Reflection Horizontal ATR accessory. The spectral range was collected between 600 and 4000 cm^{-1} with a spectral resolution of 4 cm^{-1}. 256 scans were performed to ensure the reproducibility of the data. Water was taken as background for the analysis.

2.7. In-vitro drug release studies

The in-vitro release studies were conducted at 34 °C (Ocular surface temperature). 180 μL of the formulation was placed in a dialysis membrane, which was placed in 9 mL of simulated tear fluid (STF). 3 mL aliquots were collected at regular intervals and replaced with equal amounts of fresh STF. The drugs were analyzed by the method developed by Walash et al.[43] and Maulvi et al.[44]. Malvern OmniSec system fitted with a degasser and a Discovery HS C18 column (250 mm X 4.6 mm, 5 μm) was used for the analysis. The mobile phase of 10 mM PBS and acetonitrile (50:50) was selected with a flow rate of 1 mL/min with a run time of 5 mins (found suitable for the separation after trying different concentrations and flow rates). An injection volume of 50 μL was selected. The collected drug aliquots were diluted with acetonitrile to the final ratio of 50:50 STF (with drug) and acetonitrile before analysis. The column oven and detector oven temperature were kept at 30 °C. The drug was analyzed using the UV detector in the system at 295 nm (for timolol) and 215 nm (for latanoprost).

2.8. Drug release kinetic models

2.8.1. Zero order model

The zero-order release kinetics can be defined by $Q_t = Q_0 + K_0 t$, where, Q_t is the drug released at time t, Q_0 is the initial amount of drug in the release medium (=0) and K_0 is the zero-order release constant. The cumulative amount of drug released is plotted vs time and slope of the plot is given by K_0.

2.8.2. First order model

The first-order release kinetics can be defined by $\frac{dc}{dt} = -Kc$, where, C is the concentration of drug remaining in the biomaterial, t is the time and K is the first order release constant. This can be further expressed as log $C = \log C_0 - Kt/2.303$, where, C_0 is the initial drug concentration in the biomaterial. The data are plotted as log of cumulative percentage of drug remaining vs time and slope of the plot gives -K/2.303.

2.8.3. Higuchi model

The Higuchi model is defined as $Q = K_h \times t^{1/2}$, where, Q is the drug release at time t, and k_H is the Higuchi dissolution constant. The data

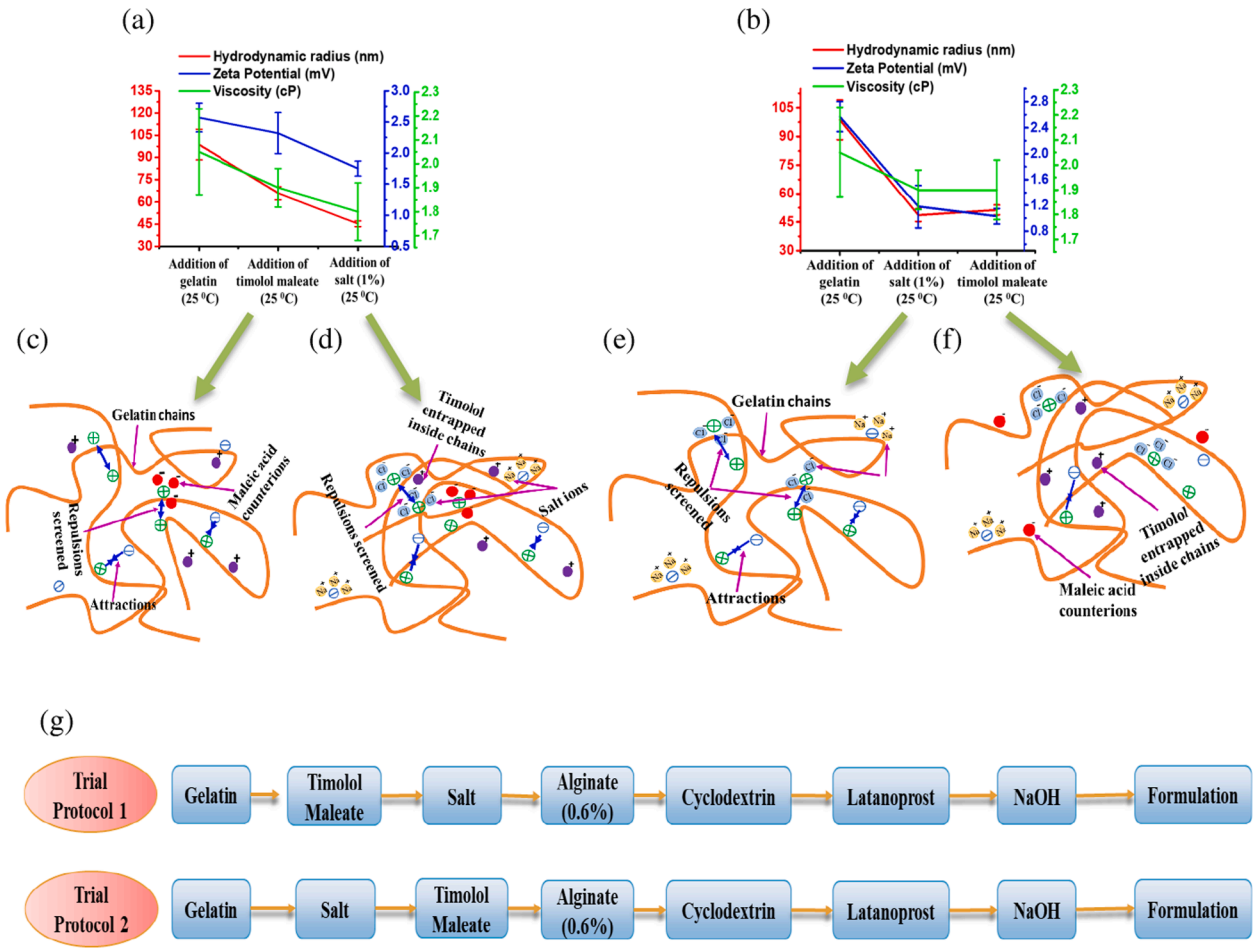

Fig. 2. Effect of the sequence of salt addition on interactions between gelatin, timolol maleate and NaCl. a) Changes in RH, zeta potential, and viscosity with the addition of timolol maleate followed by NaCl to gelatin solution, b) Changes in RH, zeta potential and viscosity with the addition of NaCl followed by timolol maleate to gelatin solution, c)A rough schematic of the interactions between timolol maleate and gelatin, d) A rough schematic of the interactions between timolol maleate, gelatin and NaCl, e) A rough schematic of the interactions between NaCl and gelatin, f) A rough schematic of the interactions between NaCl, gelatin and timolol maleate, g) Sequence of mixing components taken into consideration.

obtained are plotted as the cumulative release drug vs square root of t. The slope of this plot gives the value of K_h.

3. Results and discussions

3.1. Protocol development

Timolol maleate and latanoprost have a therapeutic action time of around 12 and 18 h, respectively. Hence, it would be beneficial to enhance timolol's action time more than latanoprost. Thus, timolol maleate needs to be loaded into the formulation early, providing an additional layer of the polymer resulting in more diffusion resistance and a delayed release.

Gelatin is a small chain (low viscosity) polymer compared to alginate in this study. It would be advantageous to include alginate after the addition of gelatin. A better drug release was reported for formulations where low-viscosity polymer was added before the high-viscosity polymer[45].

The alginate concentration was considered based on the viscosity of the formulations. Supplementary table T1 shows the viscosity of the formulations with 1% NaCl, 1% gelatin, 0.2% β-cyclodextrin, 1.65 mg/mL of timolol maleate and 1.5 μg/mL of latanoprost with varying alginate concentration. 0.6% of alginate was considered for designing the formulations as the viscosity was around 65 cP for the formulations (permissible viscosity of ophthalmic formulations) at 34 °C.

Fig. 1 (a) and (b) show the interactions between the individual polymers and timolol maleate. Timolol maleate is a maleic acid salt of timolol. Timolol has a secondary amide; thus, it is a positively charged drug molecule below its pKa of 9.76. Its addition at solution pH (gelatin solution: 5.3 ± 0.5 and alginate solution: 4.1 ± 0.5) reduces R_H and viscosity of gelatin and alginate due to their charge screening by the maleic acid counter ions leading to the collapse of the chains inferring its inability to diffuse inside the chains. The isoelectric point of gelatin is at pH 8.1 (zeta potential at pH 8.1 = 0.06 ± 0.05 mV). Since gelatin and alginate are dissolved in DI water (pH = 6.8 ± 0.5), thus, positive charges for gelatin (higher zeta potential) are reported. Alginate is a negatively charged polyelectrolyte; thus, negative zeta potential is reported for alginate. The reduction and increase in zeta potential for gelatin and alginate infer the decrease in the number of charges due to screening.

Fig. 1 (c) and (d) show the interactions between the individual polymers and latanoprost. Latanoprost is a neutral molecule. Hence, its addition to gelatin and alginate shows no change in zeta potential, respectively. However, a decrease in R_H is reported inferring its inability to diffuse inside the polymer chains. Since alginate does not have hydrophobic sites for the attachment of latanoprost (hydrophobic molecule), β – cyclodextrin can be used to encapsulate it. Cyclodextrins have a hydrophilic outer wall and a hydrophobic inner wall [46]. The addition of cyclodextrin to alginate leads to the increase in R_H, inferring its ability to diffuse inside alginate chains.

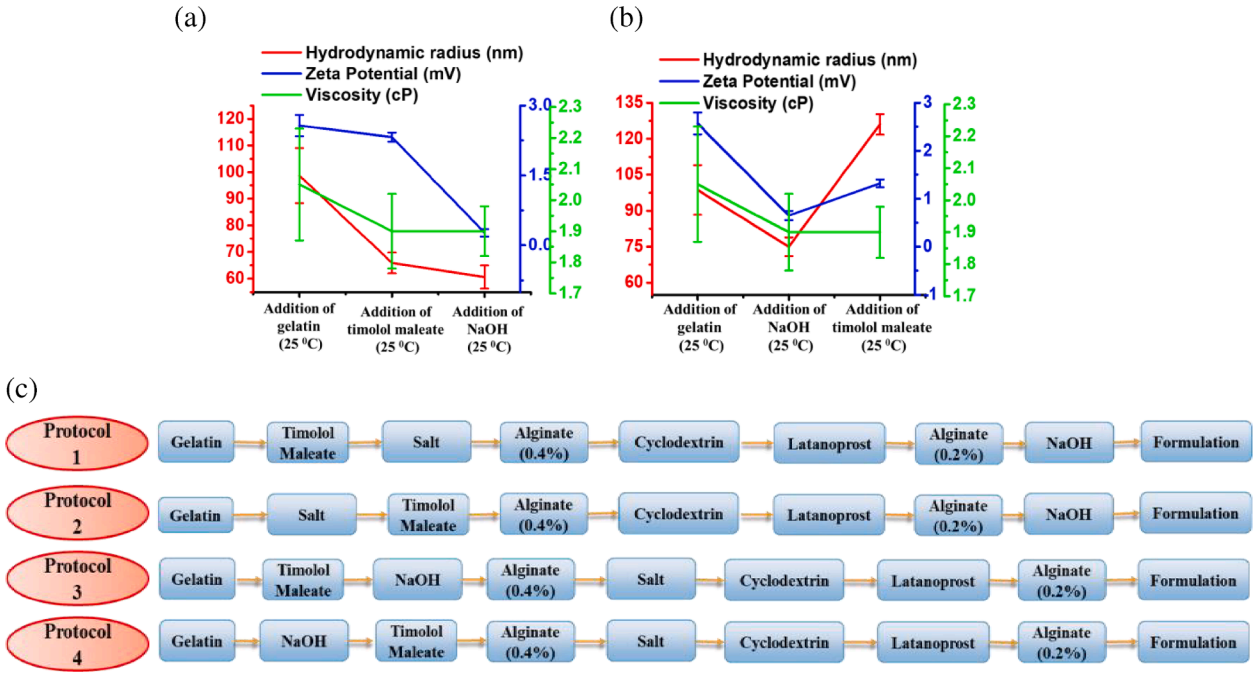

Fig. 3. Effect of the sequence of NaOH addition on interactions between gelatin, timolol maleate and NaOH. a) Changes in RH, zeta potential and viscosity with the addition of timolol maleate followed by NaOH to gelatin solution, b) Changes in RH, zeta potential and viscosity with the addition of NaOH followed by timolol maleate to gelatin solution, c) protocols taken into consideration for the formulation design.

A subsequent increase in R_H is reported with the further addition of latanoprost which infers that it can get diffused inside the alginate chains due to the addition of cyclodextrin (Fig. 1 (e)). The hydrophilic ends of cyclodextrins get attached to alginate chains, and the latanoprost gets attached to the hydrophobic, as shown in Fig. 1(f). Figure S1 shows the FTIR bands for alginate, alginate + latanoprost, and Figure S2 shows the FTIR bands for alginate, alginate + cyclodextrin, and alginate + cyclodextrin + latanoprost. The addition of latanoprost to alginate shows almost no change in the absorbance of the bands, thus justifying that latanoprost cannot interact with the chains (Figure S1). However, when cyclodextrin is added to alginate leads to an increase in the absorbance in N–H/O–H coupled band, thus, inferring an increase in H-bonds. It also shows an increase in CH_2 bands' absorbance, the favourable interaction of alginate and cyclodextrin. The addition of latanoprost shows a reduction in absorbance except for the N–H/O–H coupled band which shows an increase in absorbance, thus inferring that latanoprost could diffuse inside the chains and interact with the alginate and cyclodextrin (Figure S2). If latanoprost could not interact and diffuse, it should have shown no change in the absorbance of the bands as seen in Figure S1.

Fig. 2 (a) shows the effect of NaCl on gelatin and timolol maleate mixture on the R_H, zeta potential and viscosity. The addition of timolol maleate leads to screening some of the positive charges on the gelatin. The further addition of NaCl leads to the further reduction in R_H, zeta potential and viscosity due to screening of the remaining repulsive (positive) charges, allowing the timolol molecules to get entrapped inside the chains with the collapsed gelatin chains forming a shell around the drug molecules as shown in Fig. 2 (c) and (d).

Another possibility is the addition of timolol maleate to the gelatin and salt mixture. For this case, the addition of NaCl shows a reduction in R_H, zeta potential and viscosity of gelatin solution due to screening of the charges (Fig. 2(b)). An increase in R_H with the addition of timolol maleate is reported, which infers the expansion of the gelatin chains and hence, results in the drug molecules getting diffused inside the chains (as there are no repulsive forces available in gelatin chains hindering the timolol maleate diffusion) as shown in Fig. 2(e) and (f)).

The trial protocols (Fig. 2 (g) and interactions for these protocols shown in Figure S3) were developed based on the above-discussed interactions of salt, polymers, drugs and cyclodextrin. The addition of salt after timolol maleate will lead to the encapsulation of the drug within the gelatin chains due to the collapse of chains (with the addition of salt), which will provide extra diffusional resistance to the drug (Trial Protocol 1). The addition of timolol maleate after salt will lead to the progression of the drug inside the gelatin chains as the positive charges on gelatin chains are already screened, and hence, there are no repulsions for the positively charged drug molecules along with the screening of attractive charges from the maleic acid molecules. Thus, the drug molecules will get encapsulated within the gelatin chains (Trial Protocol 2). NaOH is added to increase the pH of the formulations to the physiological level. These protocols showed a sustained release of timolol maleate and latanoprost for 240 mins and 30 mins, respectively. A burst release for latanoprost was reported since latanoprost was added at the end of these protocols. Therefore, 0.6% alginate is divided into 0.4% and 0.2%, and the latter is added to the formulation after adding latanoprost, which provides an extra alginate layer (thus, a diffusional resistance) to latanoprost.

Protocols 1 and 2 are modified versions of the trial protocols (Fig. 3 (c)). However, NaOH is added at the end of these protocols, thus, leading to the alginate chains to an expanded state. To overcome this, NaOH could be added at an earlier stage. The NaOH required to increase the final formulation's pH to the physiological level when added to the gelatin, and the gelatin & timolol maleate mixture increases their pH to 8.2. The addition of NaOH after timolol maleate led to further collapse of chains, similar to when NaCl was added after timolol maleate (Fig. 3 (a)). The addition of timolol maleate after NaOH addition to gelatin leads to the screening of attractive forces and thus expansion of the chains, similar to when NaCl was added to the gelatin solution followed by timolol maleate (Fig. 3(b)). Hence, protocols 3 and 4 were prepared following the same rationale as protocols 1 and 2 (Fig. 3 (c)). The interactions for these protocols are shown in Figure S4.

In summary, based on the above discussions, the four protocols are designed to study the impact of different salts on this biomaterial. The salts are added in between gelatin and alginate for protocols 1 and 2 while, for protocols 3 and 4, it is added to the gelatin and alginate

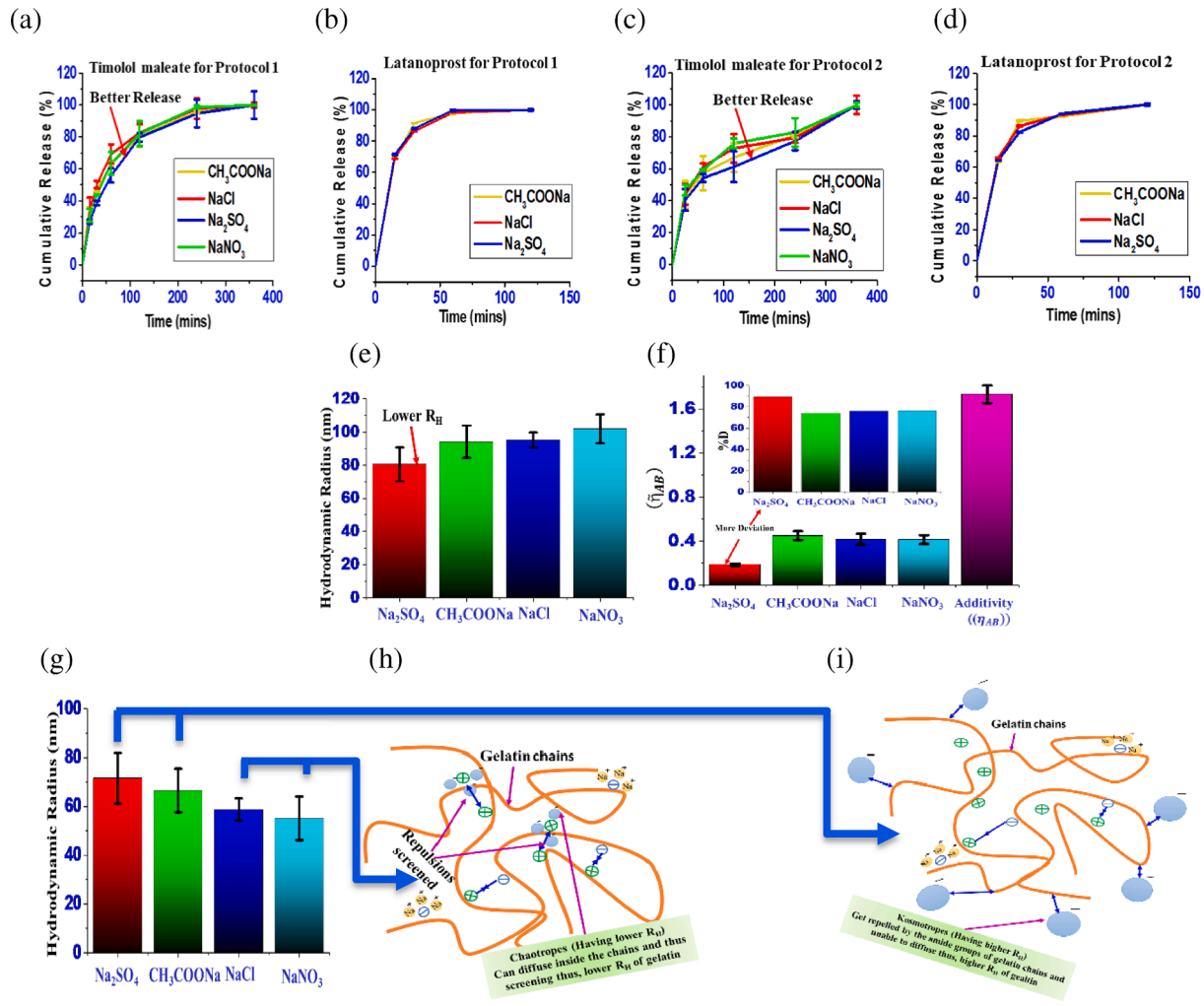

Fig. 4. Drug release and interactions of different salts for protocols 1 and 2. a) Drug release profiles for timolol maleate for protocol 1, b) Drug release profiles for latanoprost for protocol 1, c) Drug release profiles for timolol maleate for protocol 2, d) Drug release profiles for latanoprost for protocol 2, e) Variation in R_H with different salts for gelatin and alginate mixture for protocols 1 & 2, f) Variation in (η_{AB}) with different salts for gelatin and alginate mixture for protocols 1 & 2 along with the %D for the same, g) Variation in R_H with different salts for gelatin, h) A rough schematic for the interactions of chaotropes with gelatin, i) A rough schematic for the interactions of kosmotropes with gelatin.

mixture to analyze the impact of the sequence of addition. Hence, based on the sequence, the salts will first interact with the gelatin (polyampholyte) for protocols 1 and 2 and the subsequent addition of alginate to the solution will show the impact of alginate to the polyampholyte salt solution. For protocols 3 and 4, the impact of the salts on the mixture/complex of gelatin and alginate is shown.

3.2. Interactions of different salts

The interactions can be discussed using the intrinsic viscosities, which will provide another perspective on the interactions of the developed protocols, which can be used to correlate to the release profiles and R_H.

The intrinsic viscosity of the polymer solutions can be determined by the Huggins equation, which is as follows [47]

$$\frac{\eta_{sp}}{c} = [\eta] + k_H [\eta]^2 c \tag{8}$$

where, η_{sp} is the specific viscosity $= \eta_{rel}$-1, c is the concentration of the polymer and $[\eta]$ is the intrinsic viscosity. The relative viscosity of the polymer solutions should lie between 1.2 and 2.5 [48]. The intrinsic viscosity is usually calculated at zero shear rate using capillary viscometers. However, for non-Newtonian high molecular weight

Table 1
R^2 and release constant values for different models for Protocol 1.

Salt	Protocol 1 Zero-order model		First-order model		Higuchi model	
	K_0	R^2	K	R^2	K_h	R^2
Na_2SO_4	0.3549	0.8466	0.0127	0.997	6.0477	0.9827
CH_3COONa	0.3607	0.809	0.0136	0.9922	6.2439	0.9695
NaCl	0.3663	0.7931	0.0159	0.99	6.3795	0.9619
$NaNO_3$	0.3642	0.8192	0.0173	0.9862	6.2769	0.973

Table 2
R^2 and release constant values for different models for Protocol 2.

Salt	Protocol 2 Zero-order model		First-order model		Higuchi model	
	K_0	R^2	K	R^2	K_h	R^2
Na_2SO_4	0.3216	0.8753	0.00689	0.8938	5.4531	0.9843
CH_3COONa	0.3307	0.8566	0.00785	0.9006	5.6541	0.9796
NaCl	0.333	0.8368	0.00806	0.8176	5.742	0.9712
$NaNO_3$	0.3387	0.8342	0.00875	0.8595	5.8437	0.9712

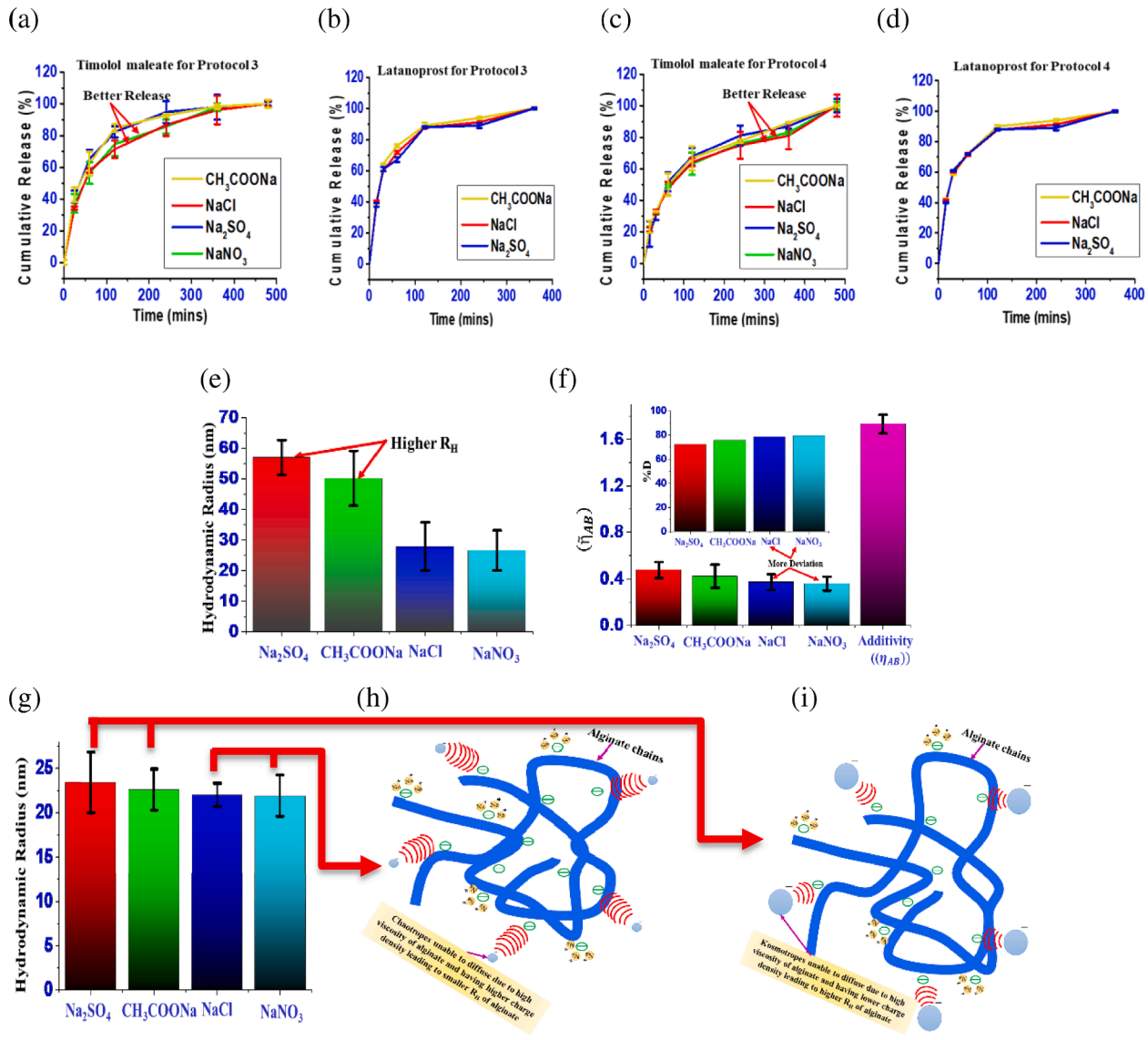

Fig. 5. Drug release and interactions of different salts for protocols 3 and 4. a) Drug release profiles for timolol maleate for protocol 3, b) Drug release profiles for latanoprost for protocol 3, c) Drug release profiles for timolol maleate for protocol 4, d) Drug release profiles for latanoprost for protocol 4, e) Variation in R_H with different salts for gelatin and alginate mixture for protocols 3 & 4, f) Variation in (η_{AB}) with different salts for gelatin and alginate mixture for protocols 3 & 4 along with the %D for the same, g) Variation in R_H with different salts for alginate, h) A rough schematic for the interactions of chaotropes with alginate i) A rough schematic for the interactions of kosmotropes with alginate.

polymers, intrinsic viscosity is a function of shear rate [49]. Thus, a shear-dependent intrinsic viscosity can be easily calculated using a rheometer [50,51]. The intrinsic viscosity is calculated from the intercept by extrapolating the plot between $\frac{\eta_{sp}}{c}$ and c to zero concentration. However, this leads to a limitation of the vanishing polymer concentration in the evaluation of viscosity data. To overcome this, a generalized intrinsic viscosity is defined as [52]

$$\{\eta\} = \frac{\partial \ln \eta_{rel}}{\partial c} \tag{9}$$

Taking into consideration the above discussion, for non-Newtonian fluids, shear-dependent generalized intrinsic viscosity (SDGIV) for high-viscosity polymer solutions, which can be calculated using a rheometer (equation 10), can be defined as.

$SDGIV\,(\eta) = \frac{\partial \ln \eta_{rel}}{\partial c}$(at a particular shear rate) (10).

Ideally, for polymer blends or mixtures, intrinsic viscosity is calculated as [53,54]

$$[\eta_{AB}] = w_A[\eta_A] + w_B[\eta_B] \tag{11}$$

where, $[\eta_{AB}]$ is the intrinsic viscosity of the polymer mixture, w_A is the weight fraction of polymer A, w_B is the weight fraction of polymer B, $[\eta_A]$ is the intrinsic viscosity of polymer A and $[\eta_B]$ is the intrinsic viscosity of polymer B. Equation (11) is valid with the assumption that there is no overlapping between the chains of the two polymers. However, this is not always true for polymer blends or mixtures [52].

However, the actual SDGIV for polymer blend/mixture

$$(\tilde{\eta}_{AB}) = \frac{\partial \ln \eta_{rel}}{\partial c_A}(at\ a\ particular\ shear\ rate\ and\ C_B) \neq (\eta_{AB}) \tag{12}$$

due to the overlapping of chains. The deviation from additivity is typically interpreted as highly favourable thermodynamic interactions between the polymer chains [52]. We define the deviation (%) from the additivity as

$$\%D = \frac{(\eta_{AB}) - (\tilde{\eta}_{AB})}{(\eta_{AB})} \times 100 \tag{13}$$

$(\tilde{\eta}_{AB})$ is evaluated for different salts in the interaction developed protocols by adding the polymers, salt and NaOH (as these components

affect the charges on the polymer system) in the same sequence as per the protocols keeping the alginate concentration constant at 0.6% and varying the concentration of gelatin from 0.2 to 1% and at 100 s^{-1} shear rate (also checked at 50 s^{-1} and 25 s^{-1}). It was calculated from the slope of the plot between $ln\,\eta_{rel}$ and C_A (Polymer A: gelatin) (equation (12)). (η_A) for gelatin is calculated from the slope of the plot between $ln\,\eta_{rel}$ and C_A by varying the concentration of gelatin. (η_B) for alginate is calculated from the slope of the plot between $ln\,\eta_{rel}$ and C_B by varying the concentration of alginate (Polymer B). (η_{AB}) is calculated from equation (11) and the deviation was calculated using equation (13). The higher %D infers more favourable thermodynamic interactions.

Fig. 4 (a), (b), (c) and (d) show the drug release profiles for protocols 1 and 2 with different salts. Na_2SO_4 shows a better profile than other salts in the case of timolol maleate. The profiles for the latanoprost show no change for different salts as the latanoprost is added to the formulations after adding the salts. The quantification for the latanoprost for $NaNO_3$ loaded formulation was not possible as $NaNO_3$ also shows the peak as of latanoprost at 215 nm.

According to the Hofmeister series, the protein precipitation ability (at the isoelectric point) will follow as $SO_4^{2-} > CH_3COO^- > Cl^- > NO_3^-$. At isoelectric point, the addition of chaotropes lead to the screening of positive and negative attractive forces of proteins. The chaotropes have lower R_H and thus, they can easily diffuse inside the protein chains when compared to kosmotropes. Thus, the chaotropes lead to higher R_H of proteins. The kosmotropes interacts less with protein chains as they are repelled by the amide backbones leading to collapse. Hence, the reverse of the trend is true in terms of the size of the protein/polymer, i.e., $SO_4^{2-} < CH_3COO^- < Cl^- < NO_3^-$ as the chaotropes (Cl^- and NO_3^-) can interact with the protein chains leading to its expansion and kosmotropes (SO_4^{2-} and CH_3COO^-) are unable to interact with the chains leading to their collapse. As discussed above, a partial or total reversal of this series occurs when positive charges are present on the polymer backbone. For positively charged polymer, the electrostatic repulsions will be screened with the addition of salts. The chaotropic anions would be easily able to diffuse inside the chains leading to more screening and thus will follow the reverse trend as $SO_4^{2-} > CH_3COO^- > Cl^- > NO_3^-$ in terms of R_H of polymer.

For protocols 1 and 2, the salts are added to positively charged gelatin chains. Hence, gelatin with SO_4^{2-} shows the highest R_H and follows the same trend of Hoffmeister series reversal for a positively charged system (Fig. 4(g)). Since, SO_4^{2-} is unable to interact with the gelatin chains due to the higher hydrodynamic radius of the anion (r_h); screening of positively charged gelatin chains is less compared to the chaotropic anions, as shown in Fig. 4 (i). Chaotropes having less anion r_h can diffuse inside the chains resulting in the screening of the repulsions and, thus, a collapse in gelatin chains (Fig. 4 (h)). Now, after the addition of alginate, a reversal in R_H is reported (Fig. 4 (e)). Interestingly, a higher %D and lesser $(\widetilde{\eta}_{AB})$ at 100 s^{-1} shear rate is also reported in the case of SO_4^{2-} which infers more favourable interactions between gelatin and alginate. The same trend for $(\widetilde{\eta}_{AB})$ is followed for 50 s^{-1} and 25 s^{-1} shear rates.

Since for SO_4^{2-}, the positive charges of gelatin are not screened; thus, the addition of negatively charged alginate leads to more charged interactions between the polymers. Hence, the drug release profiles for formulations prepared by protocols 1 and 2 having Na_2SO_4 show a better release profile than other salts because of increased interactions between the polymers. However, CH_3COONa, NaCl and $NaNO_3$ show the same release profile for timolol maleate (almost similar R_H values for gelatin and alginate mixture (Fig. 4 (e)) along with almost similar $(\widetilde{\eta}_{AB})$ and %D (Fig. 4 (f))).

Thus, from the release profile, it can be inferred that, at a particular time, the least drug is released from the formulation containing SO_4^{2-} and thus, following the series as$SO_4^{2-} < CH_3COO^- \approx Cl^- \approx NO_3^-$analogous to the R_H and $(\widetilde{\eta}_{AB})$ for the gelatin and alginate mixture. The single-factor ANOVA analysis of the data for the effect of different salt on time required for 90% release of timolol maleate for protocols 1 and 2 with 95% confidence implies an effect of salt on the drug release. However, when considering the salts except Na_2SO_4 shows no effect on the drug release, thus statistically defining $CH_3COO^- \approx Cl^- \approx NO_3^-$. No effect of salts on the latanoprost release time is also implied (Supplementary table T2).

The following Tables 1 and 2 shows the R^2 values for the data fitting with the actual data and the value of the release kinetic constants for protocols 1 and 2 respectively.

From the tables, it is evident that, for SO_4^{2-} the R^2 values are higher which essentially means, that, the release data fitting is better for SO_4^{2-} when compared to others. Hence, the drug release profile for SO_4^{2-} is better when compared to other salts and thus, explaining the series as $SO_4^{2-} < CH_3COO^- \approx Cl^- \approx NO_3^-$ in terms of drug release.

Fig. 5 (a), (b), (c), and (d) shows the drug release profiles for protocols 3 and 4. Protocols 1 and 2 show inferior release results for both drugs compared to protocols 3 and 4. For protocols 3 and 4, salt is added after alginate, leading to the collapse of alginate chains, thus explaining a better release than protocols 1 and 2, where alginate chains were relatively open. NaOH is also added at the end for protocols 1 and 2, resulting in the opening of the alginate chains which thus explains the inferior results for the latanoprost profile compared to protocols 3 and 4.

The two-way ANOVA analysis to study the impact on the protocols and different salt on the drug release infers that different salts have no effect on the drug release for both drugs. However, a significant effect is inferred for the protocol variation for both drugs (Supplementary table T3).

For protocols 3 & 4, the drug release follows the series as $SO_4^{2-} \approx CH_3COO^- > Cl^- \approx NO_3^-$. Thus, the chaotropes show a better release profile for this case. Salt is added after alginate for these cases. Now, ideally, for a negatively charged molecule, the anions will follow the actual Hoffmeister series, i.e., $SO_4^{2-} < CH_3COO^- < Cl^- < NO_3^-$. Since the chaotropes can diffuse inside the chains, they can provide some repulsions and, thus, causing in an expanded state of the chains when compared with kosmotropes which are unable to diffuse inside chains due to their higher r_h, as shown in the case of gelatin at pH 10 (negatively charged) in Figure S5.

However, in the case of alginate, this is not observed. The reversal of the series is observed for alginate (Fig. 5(g)). This may be due to the higher viscosity of the alginate solution. The electrostatic interactions of salt cannot overcome the viscous barrier of alginate chains; thus, the chaotropes and kosmotropes cannot diffuse inside the chains.

For understanding the reversal, the charge density of the ions needs to be considered. Table 3 shows the charge densities of the hydrated anions, which were calculated by modifying the ionic charge density equation by replacing the ionic charge radius with the R_H of the anions

$$C = \frac{ne}{\frac{4}{3}\pi {r_h}^3} \tag{14}$$

where C is the charge density in C/mm^3, n is the ion charge, e is the electron charge (1.6×10^{-19}C), and r_h is the anion hydrodynamic radius in mm calculated from the Stoke-Einstein equation.

Table 3
Calculated charge densities of hydrated anions.

Anions	Diffusivity (0.10^{-9} m^2/s)	r_h (0.10^{-10} m)	Charge density (C/mm^3)
SO_4^{2-}	1.060	2.57	4.5
CH_3COO^-	1.089	2.50	2.4
Cl^-	1.730	1.58	9.68
NO_3^-	1.903	1.43	13.06

The charge densities of the chaotropes are much higher than the kosmotropes. Thus, when the chaotropes cannot diffuse inside the chains, they will provide more repulsions to the alginate chains than kosmotropes. Thus, a slightly lower R_H of alginate is reported for the chaotropes when compared to kosmotropes (Fig. 5 (g) and schematics in Fig. 5 (h) and (i)). Hence, it can be inferred that, for negatively charged high-viscosity polymer systems, a Hofmeister reversal occurs which is also related with the charge densities of the anions. The same trend in R_H and $(\widetilde{\eta}_{AB})$ at 100 s^{-1} shear rate of gelatin and alginate mixture is observed for protocols 3 and 4 (Fig. 5 (e) and (f)). The same trend for $(\widetilde{\eta}_{AB})$ is followed for 50 s^{-1} and 25 s^{-1} shear rates. The %D is higher for the chaotropes, thus inferring more favourable interactions between alginate and gelatin and thus explaining a better release result for NaCl and $NaNO_3$. Hence, the drug release follows the series as $SO_4^{2-} \approx CH_3COO^- > Cl^- \approx NO_3^-$ which is analogous to the R_H and $(\widetilde{\eta}_{AB})$ for the gelatin and alginate mixture. The single-factor ANOVA analysis of the data for the effect of different salt on time required for 90% release of timolol maleate for protocols 3 and 4 with 95% confidence implies an effect of salt on the drug release. However, when considering the effect of Na_2SO_4 and CH_3COONa shows no effect on the drug release, thus statistically defining $SO_4^{2-} \approx CH_3COO^-$. Similarly, NaCl and $NaNO_3$ show no effect on the drug release, thus statistically defining $Cl^- \approx NO_3^-$ No effect of salts on the latanoprost release time is also implied (Supplementary table T2).

Tables 4 and 5 shows the R^2 values for the data fitting with the actual data and the value of the release kinetic constants for protocols 3 and 4 respectively.

From the tables, it is also evident that, for SO_4^{2-} and CH_3COO^- the R^2 values are lower than Cl^- and NO_3^- which essentially means, that, the drug release profile for Cl^- and NO_3^- is a better fit. The R^2 values of SO_4^{2-} and CH_3COO^- are comparable as well as Cl^- and NO_3^- are also comparable and hence, explaining the series as $SO_4^{2-} \approx CH_3COO^- > Cl^- \approx NO_3^-$ in terms of drug release.

Table 4
R^2 and release constant values for different models for Protocol 3.

Salt	Protocol 3 Zero-order model		First-order model		Higuchi model	
	K_0	R^2	K	R^2	K_H	R^2
Na_2SO_4	0.2769	0.8099	0.00199	0.9781	5.5482	0.9578
CH_3COONa	0.2764	0.8104	0.00199	0.9766	5.5367	0.9579
NaCl	0.2665	0.8524	0.00178	0.989	5.2589	0.9774
$NaNO_3$	0.2683	0.8475	0.00182	0.9816	5.3032	0.9755

4. Conclusion

Studying the properties and interactions can lead to a strategic formulation design used to design a dual drug alginate-based anti-glaucoma formulation. The drug release profiles with different salt anions can be interrelated to the Hofmeister interaction of the salts with polymer chains. However, the Hofmeister interaction is different for the case of polymer mixture and hence, needs to be studied to get an idea of the same. The Hofmeister reversal is also true for a negatively charged high-viscosity polyelectrolyte. It can also be concluded that the interactions of the polymers with different salt vary with addition sequences. Finally, a strategic method was developed to determine the interactions amongst the polymers in the polymer mixture in terms of shear-dependent general intrinsic viscosity ($(\widetilde{\eta}_{AB})$), which follows the same trend as the R_H of the mixture and the drug release profiles. The prepared protocols 3 and 4 showed a better release for chaotropes, and protocols 1 and 2 showed a better profile for kosmotropes. Protocols 3 and 4 show a better release result when compared among the protocols. The Hofmeister interaction for protocols 1 and 2 follows the trend as $SO_4^{2-} < CH_3COO^- \approx Cl^- \approx NO_3^-$ and protocols 3 and 4 follow the trend as $SO_4^{2-} \approx CH_3COO^- > Cl^- \approx NO_3^-$ in terms of drug release profiles, hydrodynamic radius and shear-dependent general intrinsic viscosity. Hence, for protocols 1 and 2 when the salt is added in between gelatin and alginate, the kosmotropes should be preferred for a better release profile whereas for protocols 3 and 4 when the salt is added to the gelatin and alginate mixture, the chaotropes should be preferred for a better release. This scientific endeavour can be adopted as a generic guideline for any biomaterial developed to reduce trial-and-error attempts and have enhanced control of the performance of the same. The same interaction-based approach was used to finally develop alginate and gelatin-based formulation for the ocular delivery of the anti-glaucoma dual drug, which was taken as a model system.

5. Funding sources

This study was supported by Department of Biotechnology, New Delhi, India (Project: BT/PR26978/NNT/28/1511/2017).

CRediT authorship contribution statement

Sougat Das: Conceptualization, Methodology, Validation, Formal analysis, Investigation, Writing – original draft. **Lopamudra Giri:** Validation, Resources, Writing – review & editing, Supervision. **Saptarshi Majumdar:** Conceptualization, Validation, Resources, Writing –

Table 5
R^2 and release constant values for different models for Protocol 4.

Salt	Protocol 4 Zero-order model		First-order model		Higuchi model	
	K_0	R^2	K	R^2	K_H	R^2
Na_2SO_4	0.2551	0.8572	0.00104	0.9388	4.9977	0.9829
CH_3COONa	0.2544	0.866	0.00108	0.94050.9405	4.9656	0.9862
NaCl	0.245	0.8718	0.00095	0.9578	4.7669	0.9863
$NaNO_3$	0.2472	0.8717	0.00095	0.9641	4.8113	0.987

review & editing, Supervision, Project administration.

Declaration of Competing Interest

The authors declare that they have no known competing financial interests or personal relationships that could have appeared to influence the work reported in this paper.

Data availability

No data was used for the research described in the article.

Acknowledgements

The authors acknowledge financial support from Prime Minister's Research Fellowship (PMRF).

Appendix A. Supplementary data

Supplementary data to this article can be found online at https://doi.org/10.1016/j.eurpolymj.2023.111961.

References

[1] S. Das, D. Saha, S. Majumdar, L. Giri, Imaging Methods for the Assessment of a Complex Hydrogel as an Ocular Drug Delivery System for Glaucoma Treatment: Opportunities and Challenges in Preclinical Evaluation, Mol. Pharm. 19 (2022) 733–748, https://doi.org/10.1021/acs.molpharmaceut.1c00831.
[2] Z.-Y. Wang, Q.-Z. Zhang, M. Konno, S. Saito, Sol–gel transition of alginate solution by the addition of various divalent cations: 13C-nmr spectroscopic study, Biopolymers. 33 (1993) 703–711, https://doi.org/10.1002/bip.360330419.
[3] B. Niu, J. Jia, H. Wang, S. Chen, W. Cao, J. Yan, X. Gong, X. Lian, W. Li, Y.-Y. Fan, In vitro and in vivo release of diclofenac sodium-loaded sodium alginate/carboxymethyl chitosan-ZnO hydrogel beads, Int. J. Biol. Macromol. 141 (2019) 1191–1198, https://doi.org/10.1016/j.ijbiomac.2019.09.059.
[4] S. Banerjee, S. Singh, S.S. Bhattacharya, P. Chattopadhyay, Trivalent ion cross-linked pH sensitive alginate-methyl cellulose blend hydrogel beads from aqueous template, Int. J. Biol. Macromol. 57 (2013) 297–307, https://doi.org/10.1016/j.ijbiomac.2013.03.039.
[5] N.T.T. Uyen, Z.A.A. Hamid, N.X.T. Tram, N. Ahmad, Fabrication of alginate microspheres for drug delivery: A review, Int. J. Biol. Macromol. 153 (2020) 1035–1046, https://doi.org/10.1016/j.ijbiomac.2019.10.233.
[6] V. Krishnaswami, R. Kandasamy, S. Alagarsamy, R. Palanisamy, S. Natesan, Biological macromolecules for ophthalmic drug delivery to treat ocular diseases, Int. J. Biol. Macromol. 110 (2018) 7–16, https://doi.org/10.1016/j.ijbiomac.2018.01.120.
[7] J. Zhao, L. Yao, S. Nie, Y. Xu, Low-viscosity sodium alginate combined with TiO2 nanoparticles for improving neuroblastoma treatment, Int. J. Biol. Macromol. 167 (2021) 921–933, https://doi.org/10.1016/j.ijbiomac.2020.11.048.
[8] D. Thomas, N. Mathew, M.S. Nath, Starch modified alginate nanoparticles for drug delivery application, Int. J. Biol. Macromol. 173 (2021) 277–284, https://doi.org/10.1016/j.ijbiomac.2020.12.227.
[9] S. Noreen, S.A. Ghumman, F. Batool, B. Ijaz, M. Basharat, S. Noureen, T. Kausar, S. Iqbal, Terminalia arjuna gum/alginate in situ gel system with prolonged retention time for ophthalmic drug delivery, Int. J. Biol. Macromol. 152 (2020) 1056–1067, https://doi.org/10.1016/j.ijbiomac.2019.10.193.
[10] M.G. Gupta Himanshu, M. Aqil, R.K. Khar, A. Asgar, B. Aseem, An alternative in situ gel-formulation of levofloxacin eye drops for prolong ocular retention, J. Pharm. Bioallied Sci. 7 (2015) 9–14, https://doi.org/10.4103/0975-7406.149810.
[11] Z. Liu, J. Li, S. Nie, H. Liu, P. Ding, W. Pan, Study of an alginate/HPMC-based in situ gelling ophthalmic delivery system for gatifloxacin, Int. J. Pharm. 315 (2006) 12–17, https://doi.org/10.1016/j.ijpharm.2006.01.029.
[12] Y. Liu, J. Liu, X. Zhang, R. Zhang, Y. Huang, C. Wu, In Situ Gelling Gelrite/Alginate Formulations as Vehicles for Ophthalmic Drug Delivery, AAPS PharmSciTech. 11 (2010) 610–620, https://doi.org/10.1208/s12249-010-9413-0.
[13] O. Séchoy, G. Tissié, C. Sébastian, F. Maurin, J.-Y. Driot, C. Trinquand, A new long acting ophthalmic formulation of Carteolol containing alginic acid, Int. J. Pharm. 207 (2000) 109–116, https://doi.org/10.1016/S0378-5173(00)00539-1.
[14] S. Cohen, E. Lobel, A. Trevgoda, Y. Peled, A novel in situ-forming ophthalmic drug delivery system from alginates undergoing gelation in the eye, J. Control. Release. 44 (1997) 201–208, https://doi.org/10.1016/S0168-3659(96)01523-4.
[15] H.-R. Lin, K.C. Sung, W.-J. Vong, In Situ Gelling of Alginate/Pluronic Solutions for Ophthalmic Delivery of Pilocarpine, Biomacromolecules. 5 (2004) 2358–2365, https://doi.org/10.1021/bm0496965.
[16] T. López-León, J.L. Ortega-Vinuesa, D. Bastos-González, A. Elaissari, Thermally sensitive reversible microgels formed by poly(N-Isopropylacrylamide) charged chains: A Hofmeister effect study, J. Colloid Interface Sci. 426 (2014) 300–307, https://doi.org/10.1016/j.jcis.2014.04.020.
[17] S.Z. Moghaddam, E. Thormann, Hofmeister effect on thermo-responsive poly (propylene oxide): Role of polymer molecular weight and concentration, J. Colloid Interface Sci. 465 (2016) 67–75, https://doi.org/10.1016/j.jcis.2015.11.040.
[18] J. Łuczak, M. Markiewicz, J. Thöming, J. Hupka, C. Jungnickel, Influence of the Hofmeister anions on self-organization of 1-decyl-3-methylimidazolium chloride in aqueous solutions, J. Colloid Interface Sci. 362 (2011) 415–422, https://doi.org/10.1016/j.jcis.2011.06.058.
[19] L. Abezgauz, K. Kuperkar, P.A. Hassan, O. Ramon, P. Bahadur, D. Danino, Effect of Hofmeister anions on micellization and micellar growth of the surfactant cetylpyridinium chloride, J. Colloid Interface Sci. 342 (2010) 83–92, https://doi.org/10.1016/j.jcis.2009.08.045.
[20] I.M. Heyns, R. Pfukwa, L. Bertossi, L.E. Ball, M.A. Kelland, B. Klumperman, Thermoresponsive behavior of poly(3-methylene-2-pyrrolidone) derivatives, Eur. Polym. J. 112 (2019) 714–721, https://doi.org/10.1016/j.eurpolymj.2018.10.040.
[21] B. Kalkan, N. Orakdogen, Strength and salt/pH dependent-sorption capacity modulation of N-(alkyl)acrylamide-based semi-IPN hybrid gels reinforced with silica nanoparticles, Eur. Polym. J. 173 (2022), 111296, https://doi.org/10.1016/j.eurpolymj.2022.111296.
[22] T.J. Murdoch, B.A. Humphreys, J.D. Willott, K.P. Gregory, S.W. Prescott, A. Nelson, E.J. Wanless, G.B. Webber, Specific Anion Effects on the Internal Structure of a Poly(N-isopropylacrylamide) Brush, Macromolecules. 49 (2016) 6050–6060, https://doi.org/10.1021/acs.macromol.6b01001.
[23] J.D. Willott, T.J. Murdoch, G.B. Webber, E.J. Wanless, Nature of the Specific Anion Response of a Hydrophobic Weak Polyelectrolyte Brush Revealed by AFM Force Measurements, Macromolecules. 49 (2016) 2327–2338, https://doi.org/10.1021/acs.macromol.5b02656.
[24] T.J. Murdoch, J.D. Willott, W.M. de Vos, A. Nelson, S.W. Prescott, E.J. Wanless, G. B. Webber, Influence of Anion Hydrophilicity on the Conformation of a Hydrophobic Weak Polyelectrolyte Brush, Macromolecules. 49 (2016) 9605–9617, https://doi.org/10.1021/acs.macromol.6b01897.
[25] K. Ehtiati, S.Z. Moghaddam, H.-A. Klok, A.E. Daugaard, E. Thormann, Specific Counterion Effects on the Swelling Behavior of Strong Polyelectrolyte Brushes, Macromolecules. 55 (2022) 5123–5130, https://doi.org/10.1021/acs.macromol.2c00411.
[26] R. Kou, J. Zhang, T. Wang, G. Liu, Interactions between Polyelectrolyte Brushes and Hofmeister Ions: Chaotropes versus Kosmotropes, Langmuir. 31 (2015) 10461–10468, https://doi.org/10.1021/acs.langmuir.5b02698.
[27] J.D. Willott, T.J. Murdoch, B.A. Humphreys, S. Edmondson, E.J. Wanless, G. B. Webber, Anion-Specific Effects on the Behavior of pH-Sensitive Polybasic Brushes, Langmuir. 31 (2015) 3707–3717, https://doi.org/10.1021/acs.langmuir.5b00116.
[28] Y. Yu, Y. Yao, S. van Lin, S. de Beer, Specific anion effects on the hydration and tribological properties of zwitterionic phosphorylcholine-based brushes, Eur. Polym. J. 112 (2019) 222–227, https://doi.org/10.1016/j.eurpolymj.2019.01.013.
[29] X. Wang, C. Qiao, K. Song, S. Jiang, J. Yao, Hofmeister effect on the viscosity properties of gelatin in dilute solutions, Colloids Surfaces B Biointerfaces. 206 (2021), 111944, https://doi.org/10.1016/j.colsurfb.2021.111944.
[30] T. López-León, A. Elaïssari, J.L. Ortega-Vinuesa, D. Bastos-González, Hofmeister Effects on Poly(NIPAM) Microgel Particles: Macroscopic Evidence of Ion Adsorption and Changes in Water Structure, ChemPhysChem. 8 (2007) 148–156, https://doi.org/10.1002/cphc.200600521.
[31] L. Medda, B. Barse, F. Cugia, M. Boström, D.F. Parsons, B.W. Ninham, M. Monduzzi, A. Salis, Hofmeister Challenges: Ion Binding and Charge of the BSA Protein as Explicit Examples, Langmuir. 28 (2012) 16355–16363, https://doi.org/10.1021/la3035984.
[32] M. Boström, D.F. Parsons, A. Salis, B.W. Ninham, M. Monduzzi, Possible Origin of the Inverse and Direct Hofmeister Series for Lysozyme at Low and High Salt Concentrations, Langmuir. 27 (2011) 9504–9511, https://doi.org/10.1021/la202023r.
[33] T. Oncsik, G. Trefalt, M. Borkovec, I. Szilagyi, Specific Ion Effects on Particle Aggregation Induced by Monovalent Salts within the Hofmeister Series, Langmuir. 31 (2015) 3799–3807, https://doi.org/10.1021/acs.langmuir.5b00225.
[34] B.A. Deyerle, Y. Zhang, Effects of Hofmeister Anions on the Aggregation Behavior of PEO–PPO–PEO Triblock Copolymers, Langmuir. 27 (2011) 9203–9210, https://doi.org/10.1021/la201463g.
[35] S.Z. Moghaddam, E. Thormann, The Hofmeister series: Specific ion effects in aqueous polymer solutions, J. Colloid Interface Sci. 555 (2019) 615–635, https://doi.org/10.1016/j.jcis.2019.07.067.
[36] C. Qiao, X. Wang, J. Zhang, J. Yao, Influence of salts in the Hofmeister series on the physical gelation behavior of gelatin in aqueous solutions, Food Hydrocoll. 110 (2021), 106150, https://doi.org/10.1016/j.foodhyd.2020.106150.
[37] V. Balos, H. Kim, M. Bonn, J. Hunger, Dissecting Hofmeister Effects: Direct Anion-Amide Interactions Are Weaker than Cation-Amide Binding, Angew. Chemie Int. Ed. 55 (2016) 8125–8128, https://doi.org/10.1002/anie.201602769.
[38] J. Paterová, K.B. Rembert, J. Heyda, Y. Kurra, H.I. Okur, W.R. Liu, C. Hilty, P. S. Cremer, P. Jungwirth, Reversal of the Hofmeister Series: Specific Ion Effects on Peptides, J. Phys. Chem. B. 117 (2013) 8150–8158, https://doi.org/10.1021/jp405683s.
[39] I. Giner, G. Pera, C. Lafuente, M.C. López, P. Cea, Influence of the Hofmeister series of anions on the molecular organization of positively ionized monolayers of a viologen derivative, J. Colloid Interface Sci. 315 (2007) 588–596, https://doi.org/10.1016/j.jcis.2007.06.085.
[40] N. Schwierz, D. Horinek, U. Sivan, R.R. Netz, Reversed Hofmeister series—The rule rather than the exception, Curr. Opin. Colloid Interface Sci. 23 (2016) 10–18, https://doi.org/10.1016/j.cocis.2016.04.003.

[41] N. Schwierz, D. Horinek, R.R. Netz, Reversed Anionic Hofmeister Series: The Interplay of Surface Charge and Surface Polarity, Langmuir. 26 (2010) 7370–7379, https://doi.org/10.1021/la904397v.
[42] F. Ross Hallett, Particle size analysis by dynamic light scattering, Food Res. Int. 27 (1994) 195–198, https://doi.org/10.1016/0963-9969(94)90162-7.
[43] M. Walash, R. El-Shaheny, Fast separation and quantification of three anti-glaucoma drugs by high-performance liquid chromatography UV detection, J. Food Drug Anal. 24 (2016) 441–449, https://doi.org/10.1016/j.jfda.2015.11.006.
[44] F.A. Maulvi, T.G. Soni, D.O. Shah, Extended Release of Timolol from Ethyl Cellulose Microparticles Laden Hydrogel Contact Lenses, Open Pharm. Sci. J. 2 (2015) 1–12, https://doi.org/10.2174/1874844901502010001.
[45] T. Basu, U. Bhutani, S. Majumdar, Cross-linker-free sodium alginate and gelatin hydrogels: a multiscale biomaterial design framework, J. Mater. Chem. B. 10 (2022) 3614–3623, https://doi.org/10.1039/D2TB00028H.
[46] J. HU, 8 - Environmentally sensitive polymer gel and its application in the textiles field, in: J.B.T.-S.M.P. and T. HU (Ed.), Woodhead Publ. Ser. Text., Woodhead Publishing, 2007: pp. 252–278. 10.1533/9781845693060.252.
[47] S. Panda, G.C. Mohanty, R.N. Smal, A.P. Mohapatra, M.K. Nayak, A. Acharya, G. S. Roy, Evaluation Of Huggins ' Constant, Kraemer ' s Constant And Viscosity Concentration Co-Efficient Of Polymer PVA (Mw = 1, 25, 000) In Distilled Water, 1N NaOH And 1N KOH, Researcher. 2 (2010) 5–9.
[48] W.-M. Kulicke, C. Clasen, in: The Intrinsic Viscosity BT - Viscosimetry of Polymers and Polyelectrolytes, Springer, Berlin Heidelberg, Berlin, Heidelberg, 2004, pp. 41–48, https://doi.org/10.1007/978-3-662-10796-6_4.
[49] S.L. Young, C.F. Shoemaker, Measurement of shear-dependent intrinsic viscosities of carboxymethyl cellulose and xanthan gum suspensions, J. Appl. Polym. Sci. 42 (1991) 2405–2408, https://doi.org/10.1002/app.1991.070420905.
[50] J. Liu, J. Zhang, B. Zhang, X. Zhang, L. Xu, J. Zhang, J. He, C.-Y. Liu, Determination of intrinsic viscosity-molecular weight relationship for cellulose in BmimAc/DMSO solutions, Cellulose. 23 (2016) 2341–2348, https://doi.org/10.1007/s10570-016-0967-1.
[51] H. Hu, A. Takada, Y. Takahashi, Intrinsic Viscosity of Pullulan in Ionic Liquid Solutions Studied by Rheometry, 日本レオロジー学会誌. 42 (2014) 191–196, https://doi.org/10.1678/rheology.42.191.
[52] M. Bercea, B.A. Wolf, Intrinsic Viscosities of Polymer Blends: Sensitive Probes of Specific Interactions between the Counterions of Polyelectrolytes and Uncharged Macromolecules, Macromolecules. 51 (2018) 7483–7490, https://doi.org/10.1021/acs.macromol.8b01422.
[53] W.R. Krigbaum, F.T. Wall, Viscosities of binary polymeric mixtures, J. Polym. Sci. 5 (1950) 505–514, https://doi.org/10.1002/pol.1950.120050408.
[54] L.H. Cragg, C.C. Bigelow, The viscosity slope constant k′—ternary systems: Polymer–polymer–solvent, J. Polym. Sci. 16 (1955) 177–191, https://doi.org/10.1002/pol.1955.120168208.